Investigation on the influence of fibre reinforcement on chloride induced corrosion of RC structures

Carlos G. Berrocal[1,2], Karin Lundgren[1], Ingemar Löfgren[1,2]

[1]Department of Civil and Environmental Engineering, Division of Structural Engineering, Chalmers University of Technology, SE-41296, Gothenburg, Sweden

[2]Thomas Concrete Group AB Södra Vägen 28, 412 54, Gothenburg, Sweden

Abstract

Corrosion of reinforcement is the main cause of deterioration of RC structures located in marine environments or subjected to de-icing salts. In order to delay the ingress of chlorides, such structures require the use of thick, dense concrete covers and strict crack width limitations. Given the crack limiting effect provided by fibres, it would be of interest to incorporate fibre reinforcement to conventionally reinforced concrete structures. Nevertheless, whereas fibre reinforcement might delay the penetration of detrimental agents into the concrete through crack control, there are other aspects which need to be addressed to determine whether fibres can improve the overall durability of RC structures.

Several experiments were conducted within the present project, parts of them still ongoing, to investigate some of these aspects, namely: (i) the effect of fibres on the diffusivity of uncracked concrete; (ii) whether fibres may affect the corrosion onset of rebars for any crack width; (iii) whether steel fibres, due to their conductive nature, might influence the resistivity and consequently the corrosion rate of embedded rebars; and (iv) whether there is a risk of galvanic corrosion between steel fibres and rebars.

Obtained results from chloride migration and bulk diffusion tests showed that fibres had no significant influence on the diffusion coefficient of concrete. Results from experiments in which RC beams were subjected to different loading conditions and thereafter naturally corroded through exposure to highly concentrated salt solution, showed a trend for earlier corrosion initiation with increasing crack width. Concrete mixes incorporating fibres exhibited similar or delayed corrosion onset compared to their plain concrete counterparts. While resistivity of FRC was consistently lower than resistivity of plain concrete measured under AC at 1 kHz, corrosion rate measurements based on the galvanostatic pulse technique showed no clear correlation between the presence of fibres and the corrosion rate.

1 Introduction

Over the past 50 years many studies have investigated the mechanical and fracture properties of fibre reinforced concrete. Today, fibres are often incorporated to industrial floors or slabs on grade in order to control shrinkage cracking as well as in tunnels as sprayed concrete or precast segmental linings. Furthermore, there is an increasing interest in using fibre reinforced concrete in structural applications, which has resulted in the appearance of guidelines in recently released design codes, e.g., (Model Code 2010; Swedish Standard 812310 2014).

However, owing to the casting-dependent distribution and orientation of the fibres throughout the concrete matrix, fibre reinforcement may, in many cases, be only used in combination with conventional reinforcement bars. Whereas there are available results reporting that steel fibres possess an enhanced corrosion resistance compared to traditional reinforcement (Mangat and Gurusamy 1988; Granju and Balouch 2005), the potential impact of the fibres on the corrosion process of conventional reinforcement is still unclear. Consequently, when these two types of reinforcement are combined in structures susceptible to suffer from corrosion damage, certain aspects need to be addressed to determine whether the durability of the structure would be affected.

Some of these aspects are related to the direct influence of the fibres on the mechanisms that control the corrosion process of reinforcing steel in concrete, such as chloride ingress or resistivity.- Furthermore, some consequences of adding fibre reinforcement can have an impact on rebar corrosion, such as the change of the crack pattern, with narrower and more closely spaced cracks, and a potential decrease of the degradation at the steel-concrete interface(Schiessl and Raupach 1997; Michel et al. 2013).

These aspects are currently being investigated in an ongoing project and some of the available results are presented in the following.

2 Experiments

In this project, four different concrete mixes were designed using the same concrete composition and varying the fibre type and fibre volume fraction: a) plain series which did not contain any fibres; b) steel series which incorporated 0.5% vol. of end-hooked 35 mm long steel fibres; c) hybrid series combining 0.35% vol. of steel fibres and 0.15% of 18 mm long Polyvinyl Alcohol (PVA) fibres; and d) synthetic series which contained 0.75% of 30 mm long PVA fibres.

The main part of the experimental programme carried out in this project aimed at investigating the influence of fibres, cracking, crack width and loading conditions on the corrosion process of reinforcement bars. A total of 54 beam specimens were cast, featuring dimensions of 100 × 180 × 1100 mm and reinforced with three Ø10-ribbed bars. The beams were later divided into groups according to their loading conditions: a) uncracked beams; b) unloaded beams that were pre-loaded once under three point bending to induce cracking and then unloaded; c) cyclically loaded beams that were pre-loaded with five loading-unloading cycles to cause a greater deterioration of the steel-concrete interface; and d) loaded beams that were pre-loaded to induce cracking and then reloaded with a sustained constant load. Table 1 summarizes the long-term corrosion experiments included in the experimental programme.

Table 1 Summary of long-term corrosion experiments

Load conditions			Series	Target crack widths	Quantity
Uncracked			PL	-	3
			ST	-	3
			HY	-	3
			SY	-	3
Cracked	Unloaded	1 cycle	PL	0.1, 0.2, 0.3, 0.4	4
			ST	0.1, 0.2, 0.3, 0.4	4
			HY	0.1, 0.2, 0.3, 0.4	4
			SY	0.1, 0.2, 0.3, 0.4	4
		5 cycles	PL	0.1, 0.2, 0.3, 0.4	4
			ST	0.1, 0.2, 0.3, 0.4	4
			HY	0.1, 0.2, 0.3, 0.4	4
	Loaded		PL	0.1, 0.2, 0.3, 0.4	4
			ST	0.1, 0.2, 0.3, 0.4	4

PL = Plain ST = Steel HY = Hybrid SY = Synthetic

After inducing cracking, the beams were subjected to cycles of two weeks of immersion in 10% chloride solution followed by two weeks of air drying. Fig 1 shows the experimental setup. More details about the concrete mix composition, the fibre characteristics and the geometry of the specimens can be found in (Berrocal et al. 2015).

The corrosion monitoring was divided into two phases according to Tuutti's model of reinforcement corrosion (Tuutti 1982): (i) monitoring of half-cell potential using a MnO_2 Embedded Reference Electrode (ERE) to determine the end of the corrosion initiation phase of the reinforcement bars and (ii) estimation of the corrosion rate during the propagation phase using a handheld device named RapiCor based on the galvanostatic pulse technique (Tang, Fu, and León 2010).

In addition to the long-term corrosion experiments, material tests were carried out to assess the influence of fibres on some of the mechanisms controlling the corrosion process of steel in concrete, namely the ingress of chloride ions and the electrical resistivity of concrete.

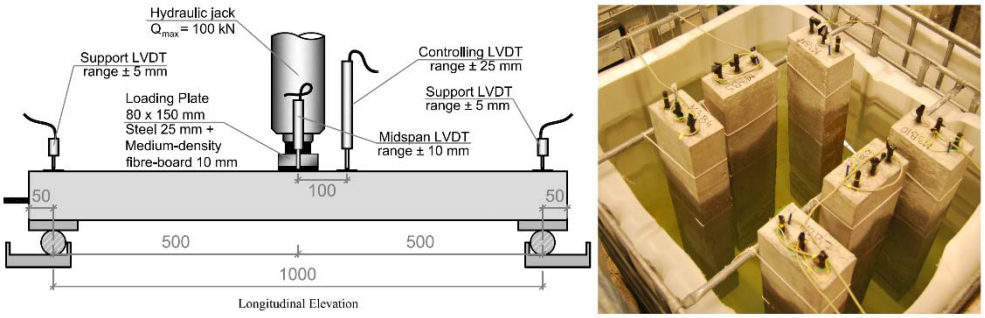

Fig. 1 Pre-loading setup used to induce cracking to the long-term corrosion beam specimens (left) and disposition of the specimens during cyclic immersion in 10% Cl solution (right).

The resistance to chloride ingress of the concrete mixes was tested according to two different standard tests: (i) chloride migration coefficient from non-steady state migration experiments according to (NT Build 492 1999), where the specimens were subjected to a constant DC voltage for 24 hours after seven weeks of water curing, and (ii) chloride diffusion coefficient from accelerated chloride penetration test according to (NT Build 443 1995), where natural diffusion tests in which the specimens were immersed in 10% chloride solution for a period of 211 days, were carried out 30 weeks after casting. The electrical resistivity of concrete was assessed using a uniaxial electrode configuration as described in (Tang, Nilsson, and Basheer 2012). The specimens used were Ø100 × 50 mm discs which were preconditioned in saturated $Ca(OH)_2$ solution for 18 hours after three hours in vacuum conditions. The electrical resistance of the samples was measured using a LCR meter under an alternate current at a frequency of 1 kHz, from which the resistivity was determined through the geometry-dependent cell constant.

3 Results and discussion

3.1 Resistance to chloride ingress and electrical resistivity of concrete

A comparison of the calculated migration coefficient from the non-steady state migration tests and the diffusion coefficient from the accelerated penetration tests as well as the electrical resistivity determined for the different concrete mixes are presented in Fig. 2. As observed, the fibres did not significantly alter the resistance to chloride ingress of uncracked concrete, with minor differences that fall within the typical coefficient of variation of the test method (typically 15% according to (Tang, Nilsson, and Basheer 2012). On the other hand, a significant reduction was observed in the electrical resistivity for the mixes with fibres and particularly for those with steel fibres. This result is in agreement with the work by (Hixson et al. 2003), who found that the insulating role of the high-impedance passive film formed around the fibres embedded in concrete disappears under AC fields or large DC potential gradients as the film can be short-circuited, thereby making the fibres conductive.

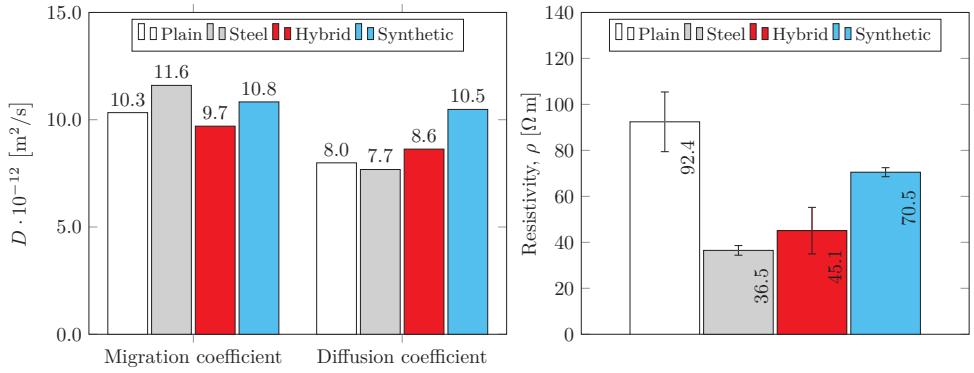

Fig. 2 Resistance of concrete to chloride ingress according to non-steady state migration tests and accelerated penetration tests (left) and resistivity measured under a 1 kHz AC field (right).

3.2 Corrosion initiation time and corrosion rate

3.2.1 Uncracked specimens

In Fig. 3 (left), a sample of half-cell potentials monitored hourly over a period of two years is presented. The displayed curves clearly show the point in time when the initiation phase ends as a sudden drop of half-cell potential, preceded by a period of relatively constant readings and followed by a succession of ups and downs coinciding with the wetting-drying cycles. Fig. 3 (right) shows the average corrosion initiation times determined for the uncracked beams. Only a marginal improvement was observed for the steel series with respect to the plain series in average terms, although a significant delay in corrosion initiation was achieved for the synthetic and particularly for the hybrid series. These results are to some degree in contradiction with the results obtained for the chloride diffusion tests, which might be attributed to a higher efficiency of the fibre reinforcement in the hybrid series (short fibres) and synthetic series (higher fibre dosage) to control restraint micro-cracks at the rebars stemming from shrinkage.

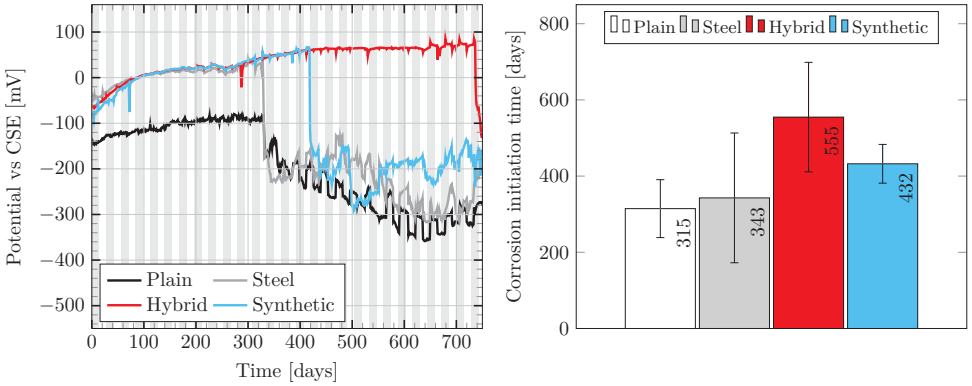

Fig. 3 Half-cell potential of reinforcing bars in uncracked specimens monitored for a period of two years (gray-shaded areas indicate immersion periods) (left) and average corrosion initiation time of reinforcement in uncracked concrete for all the mixes investigated (right).

The average cumulative cross-sectional loss estimated from corrosion rate measurements based on Faraday's law and assuming uniform corrosion is shown in Fig. 4 for the different mixes and for uncracked specimens. The results suggest that the plain series is predicted to have the lowest rebar cross-sectional loss during the period investigated, while the steel series exhibited the greatest loss, up to five times higher.

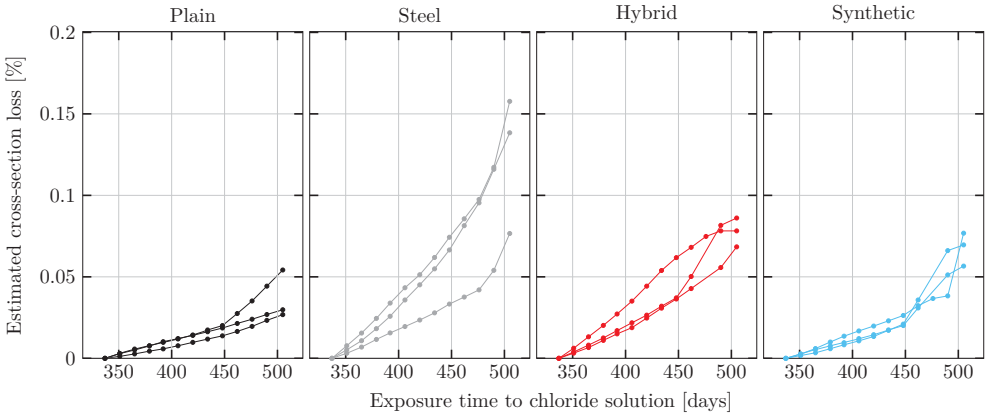

Fig. 4 Cumulative cross-sectional loss estimated from corrosion rate measurements carried out using the galvanostatic pulse technique for uncracked specimens. Each data point represents the average of four measurements performed at different locations of the same specimen.

However, it is worth noting that the hybrid series exhibited a higher corrosion rate than the plain series, even in the beginning of the investigated period, despite corrosion should have not started for the former according to the half-cell potential readings. This finding suggests that the setup of the device used to perform the corrosion rate determination, originally intended for reinforcement embedded in plain concrete, might be affected by the presence of steel fibres. If corroding steel fibres at the concrete cover can influence the results to some extent, the steel loss estimated for the steel series might actually be lower. Nevertheless, these results need to be compared with actual steel loss measurements to verify whether the trend observed holds.

3.2.2 Cracked specimens

Similar to the previous section, Fig. 5 (left) shows an example of the half-cell potential monitored for a period of two years after starting the cyclic exposure to chloride solution, corresponding to the unloaded beams with a target crack width of 0.1 mm. In Fig. 5 (right), the corrosion initiation times for each loading condition are presented, in which individual markers represents the average value of the two reinforcement bars monitored in each beam and the size of the markers correspond to the target crack width aimed during the preloading procedure.

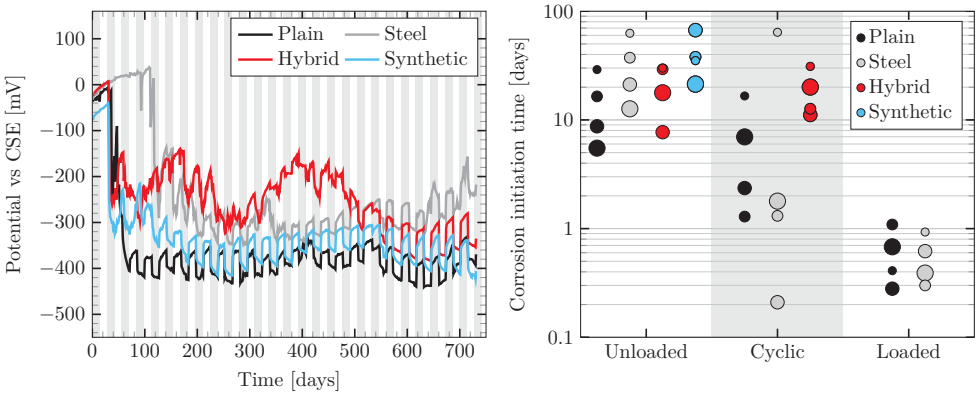

Fig. 5 Half-cell potential of reinforcing bars in unloaded specimens with target crack width of 0.1 mm monitored for a period of two years (gray-shaded areas indicate immersion periods) (left) and average corrosion initiation time of reinforcement in all cracked concrete specimens for all mixes investigated (marker size indicates the target crack width of the specimen ranging from 0.1 mm, smallest, to 0.4 mm, largest.) (right).

These results show the great impact of the loading conditions, with differences of up to two orders of magnitude between specimens unloaded and specimens subjected to sustained load. Comparing to Fig. 3 (right), the importance of the presence of cracks on the initiation period is also clear, as uncracked beams remained free of any sign of corrosion for periods more than three times longer than cracked beams. As for the influence of the fibres, only a slight improvement could be observed in some cases which was more notable in the case of the synthetic unloaded beams, whereas a somewhat negative effect could be observed in the steel cyclically loaded beams.

The role of the crack width could not be clearly identified. For the loaded beams, the results suggested the existence of a crack width threshold above which the initiation phase can be in practice disregarded. This threshold, found to be around 0.1 mm in this investigation, is most likely dependent on the concrete cover and the *w/c* ratio and therefore might not be directly extrapolated to real structures. For the unloaded and cyclically loaded beams, the variation in the initiation times could not be related to the target crack width since most of the surface crack widths ranged between 0.02 and 0.06 mm after unloading. That indicated, however, that another factor may have a larger impact on the corrosion initiation than surface crack width, e.g. small defects near the reinforcement or the interfacial damage between the concrete and the bars caused during loading, as proposed by others (Pease et al. 2010; Silva 2013; Angst et al. 2011).

In Fig. 6, the estimated cumulative cross-sectional loss for all cracked specimens is presented through a group of plots in which the columns represent the increasing target crack widths and the rows represent the different loading conditions, unloaded, cyclically loaded and loaded, as indicated in the

figure. It must be noted that the cyclically loaded specimen in the steel series with crack width 0.4 mm and the loaded specimen in the plain series with crack width 0.3 mm, both presenting cross-sectional losses of about 1.8% and 2.0%, respectively, featured cracks which greatly exceeded the intended target crack widths.

Note also that the cumulative steel loss was integrated over a longer period of time for loaded specimens since corrosion rate measurements were initiated earlier.

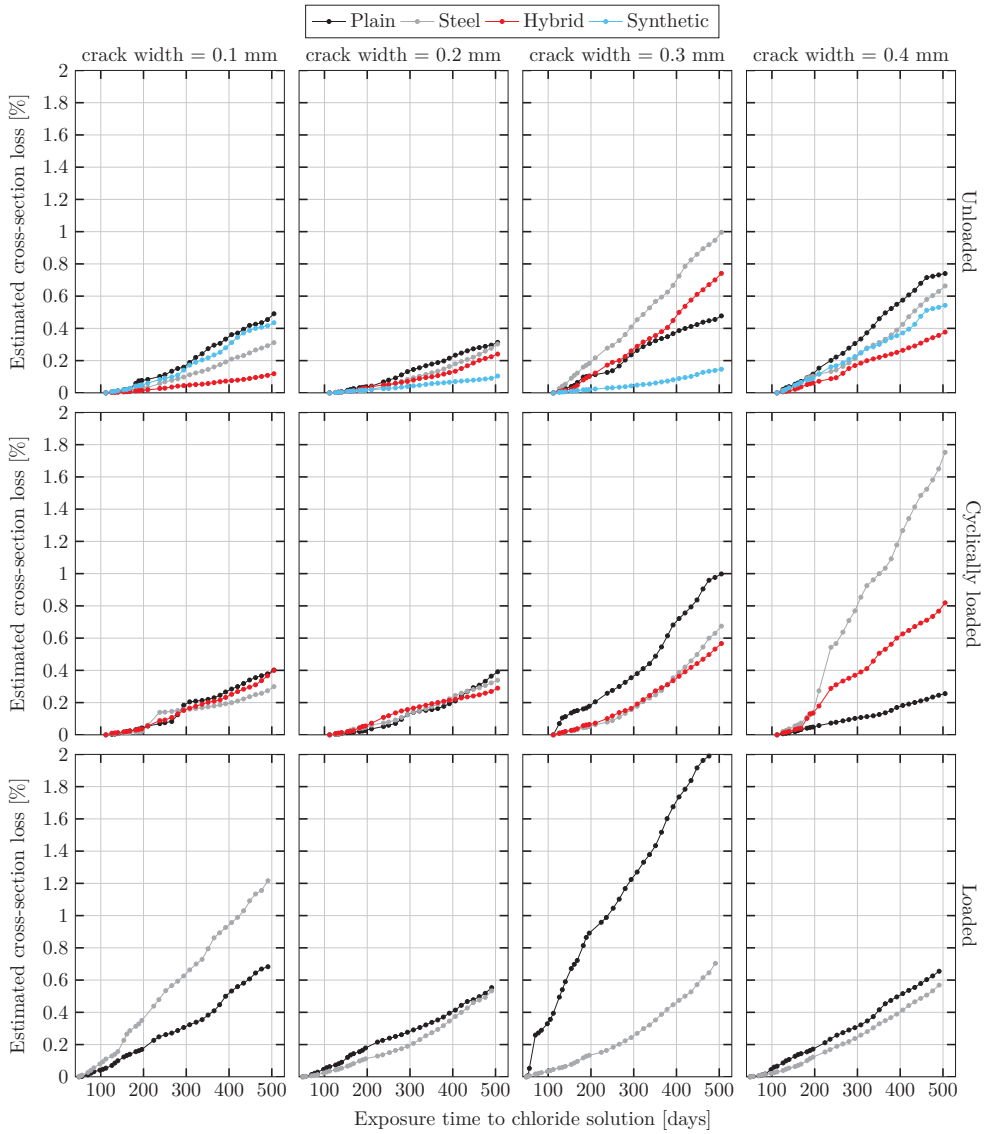

Fig. 6 Cumulative cross-sectional loss estimated from corrosion rate measurements carried out using the galvanostatic pulse technique for cracked specimens. Each data point represents the average of four measurements performed at different locations of the same specimen.

Regarding the effect of fibres, unlike for uncracked specimens where fibre reinforced mixes consistently showed higher steel loss rates, no clear effect of the fibres on the corrosion rate could be observed for the cracked specimens irrespective of the fibre type, the crack width or the loading conditions.

Looking at the results of the specimens with sustained load, no clear correlation can be stablished between the surface crack width and the rate of cross-section loss. Furthermore, some of the unloaded and cyclically loaded specimens with surface cracks of no more than 0.06 mm after closing, exhibited higher rates of steel loss than loaded specimens with open cracks of up to 0.4 mm at the surface. Thus, it is apparent that the surface crack width was not the factor controlling the corrosion rate. However, for the unloaded and cyclically loaded specimens, a qualitative change in the cross-section loss can be appreciated for beams exceeding a target crack width of 0.2 mm.

As occurred with the determination of the initiation times, the hypothesis that a greater level of internal cracking, interfacial damage (slip and separation) or small defects located along the reinforcement may have a higher impact on the corrosion rate than surface crack width, could explain the results presented in Fig. 6. Nevertheless, both the estimated cross-sectional loss and the potential relation between corrosion rate and internal damage need to be verified with gravimetric measurements of the actual steel loss and inspection of the reinforcement-concrete interface, respectively.

4 Conclusions

In this paper, partial results of an ongoing study aimed at investigating the influence of combining low dosages of fibre reinforcement with conventional reinforcing bars on corrosion induced by chloride attack have been presented. Various concrete mixes featuring different configurations of fibre reinforcement were employed to perform material tests and a long-term experiment with reinforced concrete beams in which the influence of increasing crack widths and different loading conditions have been considered.

Only minor variations were observed in the resistance of the different concrete mixes to the ingress of chloride ions, tested according to two different standard procedures, indicating a negligible influence of the fibres on the chloride diffusion coefficient of concrete. However, a certain prolongation of the corrosion initiation phase was found for uncracked beams made of fibre reinforced mixes according to half-cell potential measurements. A plausible explanation might be the arrested growth of small restraint cracks around the reinforcement. This beneficial effect of the fibres was less apparent in pre-cracked specimens, in which the loading conditions played a more important role for the corrosion initiation.

As for the corrosion propagation phase, the addition of fibres revealed a significant decrease of the concrete resistivity, which is regarded in the literature as a fundamental parameter controlling the corrosion rate of reinforcement in non-submerged cracked concrete. Whereas the corrosion rate estimated in uncracked specimens was in agreement with the resistivity measurements, specimens which remained passive according to half-cell potential monitoring exhibited higher corrosion rates than specimens in which active corrosion had already initiated. This observation might indicate a possible incompatibility of the fibres with the technique used to estimate the corrosion rate. On the other hand, the corrosion rate measurements of pre-cracked specimens did not indicate a clear influence of fibre reinforcement.

The results presented also support the hypothesis that the width of surface cracks is not the factor governing the overall corrosion process but rather internal cracking, local defects and the condition of the concrete-reinforcement interface might have a more relevant influence.

References

Angst, Ueli, Anders Rønnquist, Bernhard Elsener, Claus K. Larsen, and Øystein Vennesland. 2011. "Probabilistic Considerations on the Effect of Specimen Size on the Critical Chloride Content in Reinforced Concrete." *Corrosion Science* 53 (1) (January): 177–187. doi:10.1016/j.corsci.2010.09.017.

Berrocal, Carlos G., Ingemar Löfgren, Karin Lundgren, and Luping Tang. 2015. "Corrosion Initiation in Cracked Fibre Reinforced Concrete: Influence of Crack Width, Fibre Type and Loading Conditions." *Corrosion Science* 98 (June): 128–139. doi:10.1016/j.corsci.2015.05.021.

Granju, Jean-Louis, and Sana Ullah Balouch. 2005. "Corrosion of Steel Fibre Reinforced Concrete from the Cracks." *Cement and Concrete Research* 35 (3) (March): 572–577. doi:10.1016/j.cemconres.2004.06.032.

Hixson, A.D., L.Y. Woo, M.A. Campo, and T.O. Mason. 2003. “The Origin of Nonlinear Current–voltage Behavior in Fiber-Reinforced Cement Composites.” *Cement and Concrete Research* 33 (6) (June): 835–840. doi:10.1016/S0008-8846(02)01062-1.

Mangat, P.S., and Kribanandan Gurusamy. 1988. “Corrosion Resistance of Steel Fibres in Concrete under Marine Exposure.” *Cement and Concrete Research* 18: 44–54.

Michel, Alexander, Anders Ole Stubbe Solgaard, Brad J. Pease, Mette Rica Geiker, Henrik Stang, and John Forbes Olesen. 2013. “Experimental Investigation of the Relation between Damage at the Concrete-Steel Interface and Initiation of Reinforcement Corrosion in Plain and Fibre Reinforced Concrete.” *Corrosion Science* 77 (December): 308–321. doi:10.1016/j.corsci.2013.08.019.

Model Code. 2010. *Fib Model Code for Concrete Structures. Structural Concrete*. Vol. 14. Weinheim, Germany: Wiley-VCH Verlag GmbH & Co. KGaA. doi:10.1002/9783433604090.

NT Build 443. 1995. “North Test BUILD 443 - Accelerated Chloride Penetration.”

NT Build 492. 1999. “North Test BUILD 492 - Chloride Migration Coefficient from Non-Steady-State Migration Experiments.”

Pease, Brad, Mette Geiker, Henrik Stang, and Jason Weiss. 2010. “The Design of an Instrumented Rebar for Assessment of Corrosion in Cracked Reinforced Concrete.” *Materials and Structures* 44 (7) (December 14): 1259–1271. doi:10.1617/s11527-010-9698-1.

Schiessl, Peter, and Michael Raupach. 1997. “Laboratory Studies and Calculations on the Influence of Crack Width on Chloride-Induced Corrosion of Steel in Concrete.” *ACI Materials Journal* 94 (1): 56–61.

Silva, Nelson. 2013. “Chloride Induced Corrosion of Reinforcement Steel in Concrete. Threshold Values and Ion Distributions at the Concrete-Steel Interface.” Chalmers University of Technology, Gothenburg, Sweden.

Swedish Standard 812310. 2014. *Svensk Standard 812310:2014 Fiberbetong - Dimensionering Av Fiberbetongskonstruktioner*. Stockholm, Sverige: Swedish Standards Institute.

Tang, Luping, Ying Fu, and Alberto León. 2010. “Rapid Assessment of Reinforcement Corrosion in Concrete Bridges.”

Tang, Luping, Lars-Olof Nilsson, and P. A. Muhammed Basheer. 2012. *Resistance of Concrete to Chloride Ingress Testing and Modelling*. Spon Press.

Tuutti, Kyösti. 1982. “Corrosion of Steel in Concrete.” *CBI Report 4:82, The Swedish Cement and Cocnrete Institute.*: 468.